Structure
Article

Structural Basis of Mannan-Binding Lectin Recognition by Its Associated Serine Protease MASP-1: Implications for Complement Activation

Alexandre R. Gingras,[1] Umakhanth Venkatraman Girija,[2] Anthony H. Keeble,[2] Roshni Panchal,[2] Daniel A. Mitchell,[3] Peter C.E. Moody,[1] and Russell Wallis[1,2,*]
[1]Department of Biochemistry, University of Leicester, Leicester, LE1 9HN, UK
[2]Department of Infection, Immunity and Inflammation, University of Leicester, Leicester, LE1 9HN, UK
[3]Warwick Medical School, University of Warwick, Coventry, CV2 2DX, UK
*Correspondence: rw73@le.ac.uk
DOI 10.1016/j.str.2011.08.014

SUMMARY

Complement activation contributes directly to health and disease. It neutralizes pathogens and stimulates immune processes. Defects lead to immunodeficiency and autoimmune diseases, whereas inappropriate activation causes self-damage. In the lectin and classical pathways, complement is triggered upon recognition of a pathogen by an activating complex. Here we present the first structure of such a complex in the form of the collagen-like domain of mannan-binding lectin (MBL) and the binding domain of its associated protease (MASP-1/-3). The collagen binds within a groove using a pivotal lysine side chain that interacts with Ca^{2+}-coordinating residues, revealing the essential role of Ca^{2+}. This mode of binding is prototypic for all activating complexes of the lectin and classical pathways, and suggests a general mechanism for the global changes that drive activation. The structural insights reveal a new focus for inhibitors and we have validated this concept by targeting the binding pocket of the MASP.

INTRODUCTION

The lectin pathway of complement provides primary protection against invading pathogens. It is initiated by mannan-binding lectin (MBL) or serum ficolins, which bind to carbohydrates on pathogens to activate MBL-associated serine proteases (MASPs), leading to complement-induced lysis and stimulation of inflammatory and adaptive immune responses (Schwaeble et al., 2002). Common polymorphisms in MBL and MASPs lead to immunodeficiencies (Garred et al., 1997; Neth et al., 2001; Sumiya et al., 1991), increased severity of inflammatory disorders (Kilpatrick, 2002), and are risk factors in a number of clinical settings (Mullighan et al., 2008). Recent studies have shown that inhibition of the lectin pathway confers considerable protection toward myocardial and gastrointestinal ischemia/reperfusion injury (Schwaeble et al., 2011), so selective inhibitors will provide important therapeutic benefits.

MBLs and ficolins have bouquet-like structures formed of collagen-like stems that are linked at one end (the base) and splay apart at the other to terminate in clusters of pathogen-recognition domains (Drickamer and Taylor, 1993; Fujita et al., 2004). They circulate as complexes with three different zymogen MASPs (MASP-1 to -3) that autoactivate upon binding to pathogen-associated molecular patterns. MASPs recognize a short motif in the collagen-like stems of MBL, comprising OGKXGP (see Figure S1 available online), where the lysine is essential, O is hydroxyproline, and X is generally an aliphatic or methionine residue (Girija et al., 2007; Wallis et al., 2004). They comprise two N-terminal CUB domains (for complement C1r/C1s, Uegf, and Bmp1) each containing a binding site for MBL, separated by an epidermal growth factor (EGF)-like domain, which together form an antiparallel dimer (Wallis and Dodd, 2000). These are followed by two complement control modules (CCP) and a C-terminal serine protease (SP) domain, which control substrate recognition and catalysis (Dobó et al., 2009; Harmat et al., 2004). As well as activating complement, components participate in clearance of apoptotic cells (Botto et al., 1998), coagulation (Gulla et al., 2010; Krarup et al., 2007), inflammation (Megyeri et al., 2009), and development (Rooryck et al., 2011).

The lectin pathway of complement is similar to the classical pathway, where C1q substitutes for MBL and homologous proteases C1r and C1s replace MASPs (Wallis et al., 2010). Complexes have similar architectures, associate through analogous Ca^{2+}-dependent interactions, and activate complement via comparable mechanisms. Knowledge of the molecular basis of activation is lacking, primarily because the way in which components bind to each other is not known. To address this shortfall, we have determined the structure of components of the activating complex of the lectin pathway. The data explain how binding partners assemble and elucidate the essential role of Ca^{2+}, revealing major differences from previous predictions. Moreover, by combining the various structures that are now available, it is possible to develop a general mechanism for the physical changes in complexes that lead to complement activation.

RESULTS

Structural and Biochemical Characterization of Binding Partners

Despite intensive efforts over many years, attempts to determine a high-resolution structure of a lectin or classical pathway

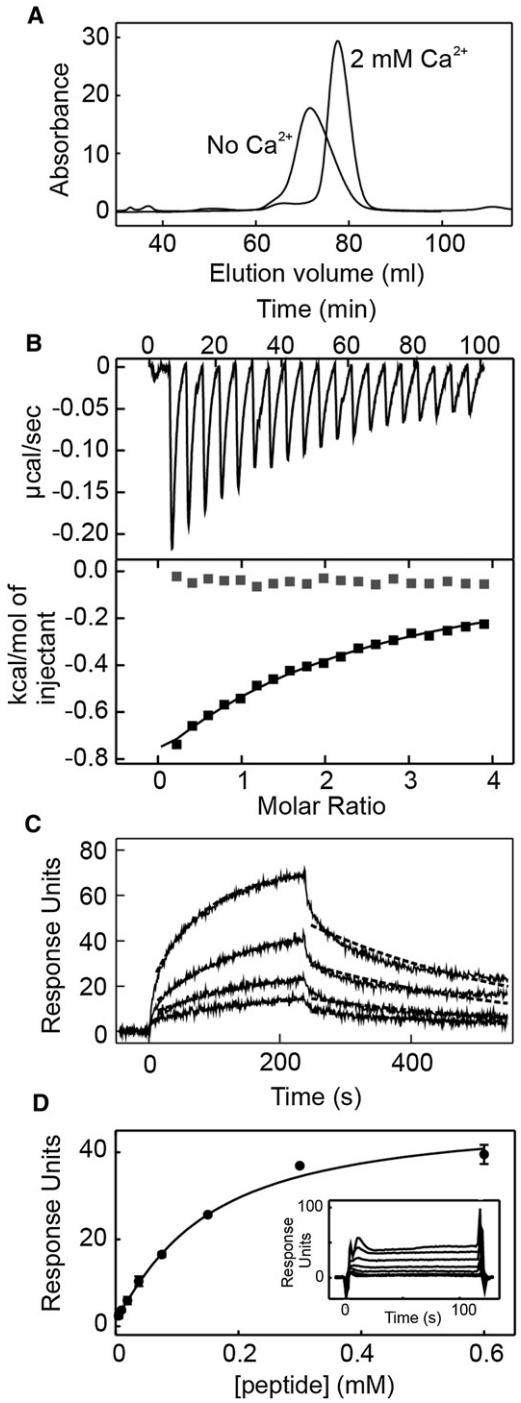

Figure 1. MASP-1 CUB2 binding to Ca^{2+} and MBL

(A) Gel filtration (Superdex 200; 16 mm/600 mm) of MASP-1 CUB2 (0.2 mg) in the presence and absence of 2 mM $CaCl_2$.

(B) Isothermal titration calorimetry of Ca^{2+} binding to MASP-1 CUB2. A representative experiment showing the energy released as $CaCl_2$ is added to the CUB2 domain (black) or buffer (gray). $K_D = 0.49 \pm 0.01$ mM and $\Delta H = -4.6 \pm 0.6$ kcal/mol in two independent experiments.

(C) Binding of MASP-1 CUB2 to MBL using surface plasmon resonance. CUB2 was injected at 20, 10, 5, and 2.5 µM and data were fitted to a 1:1 binding model in which $k_{on} = 131 \pm 13\ M^{-1}s^{-1}$ and $k_{off} = 3.5 \pm 0.3 \times 10^{-3}\ s^{-1}$ in two independent experiments.

(D) Binding of peptide 1 to MASP-1 CUB2 using surface plasmon resonance. Error bars represent the difference between duplicate measurements. The K_D was 125 ± 17 µM in two separate experiments.

complex have been unsuccessful, probably as a result of the heterogeneity of components and their intrinsic flexibility. We therefore focused on the smallest binding unit common to both pathways: a CUB domain bound to a collagen-like stem. The CUB2 domain of MASP-1/-3 (subsequently called MASP-1 CUB2) was expressed in *Escherichia coli*, refolded, and purified. It eluted significantly later from a gel filtration column in presence of Ca^{2+}, both confirming Ca^{2+} binding and suggesting that the bound form is more compact (Figure 1A). Isothermal titration calorimetry yielded a K_D of 0.5 mM for Ca^{2+}, consistent with the site being mostly occupied under physiological conditions in plasma, where the Ca^{2+} concentration is typically ~2.5 mM (Figure 1B) (Hurwitz, 1996). As anticipated, binding to MBL was weak with an apparent K_D of 27 µM (Figure 1C) compared to full-size MASP-1 (K_D ~10 nM), where multiple interactions contribute simultaneously (Chen and Wallis, 2001; Girija et al., 2007).

We determined the crystal structure of the CUB2 domain in three different conditions (Table 1). It is a β sandwich comprising nine β strands, β2–β10, linked by loops L1–L9, and with interchain disulfide bonds connecting loop L1 to strand β4 and loop L5 to loop L7. Ca^{2+} is bound at one end, sandwiched between loops L5 and L9 (Figure 2A). Six coordinating ligands to the Ca^{2+} are arranged in a tetragonal bipyramid via the side chains of Glu216, Asp226, Asp263, the main chain of Ser265 and two water molecules (Figure 3B). Ca^{2+} stabilizes loops L5 and L9 in comparison with the apo-structure of MASP-2 (Feinberg et al., 2003), in which much of loop L5 is disordered, accounting for the more compact structure shown by gel filtration (Figure 2C).

We designed two collagen-like peptides containing the binding motif of MBL at the center. Peptide 1 bound to MASP-1 CUB2 with a K_D of 125 µM (Figure 1D). The crystal structure of both uncomplexed peptides was determined and peptide 1 is shown in Figure 2B. It is a straight right-handed collagen-like triple helix, ~12 Å in diameter with the chains having a characteristic stagger, such that each residue has a unique chemical environment. The side chains of Lys46 and Leu47 point into the solvent with Lys46 of the leading chain showing nice density up to the Cε atom, as a consequence of stacking against Hyp44 of the trailing chain. In contrast, the side chains of Lys46 in the other two chains do not make intrachain contacts and are relatively poorly resolved.

Structure of the Lectin Pathway Complex

Crystals of MASP-1 CUB2 in complex with peptide 1 were grown in the presence of Ca^{2+} and diffracted to 1.8 Å resolution (Figure 3A and Table 1). The MASP binds to two of the three OGKLGP motifs in the collagen peptide (Figure 3D) with the leading and trailing chains accounting for 56% and 44% of the buried interface, respectively; the middle chain does not contact the MASP (Table 2). The side chain of Lys46 of the leading strand penetrates the MASP to contact three of the residues that also coordinate the Ca^{2+}, the carboxylate groups of Glu216 and Asp263 and the hydroxyl group of Ser265 (Figure 3C), which

Table 1. Data Collection and Refinement Statistics

	CUB2-Form 1	Peptide1	Peptide2	Complex	CUB2-Form 3	CUB2-Form 2	CUB2/ Methylamine	CUB2/ Ethylamine
Data collection								
Space group	$P4_12_12$	C2	C2	$P2_12_12$	C2	$P2_13$	$P2_13$	$P2_13$
Cell dimensions								
a, *b*, *c* (Å)	36.7, 36.7, 168.6	85.3, 23.7, 26.9	84.9, 23.4, 25.8	61.2, 52.6, 57.8	111.7, 64.7, 52.4	100.5, 100.5, 100.5	100.6, 100.6, 100.6	100.5, 100.5, 100.5
α, β, γ (°)	90.0, 90.0, 90.0	90.0, 94.1, 90.0	90.0, 94.0, 90.0	90.0, 90.0, 90.0	90.0, 92.3, 90.0	90.0, 90.0, 90.0	90.0, 90.0, 90.0	90.0, 90.0, 90.0
Resolution (Å)[a]	30–1.5 (1.6–1.5)	50–1.5 (1.58–1.5)	50–1.5 (1.59–1.5)	30–1.8 (1.9–1.8)	50–2.75 (2.9–2.75)	50–1.5 (1.59–1.5)	50–1.7 (1.8–1.7)	30–1.45 (1.54–1.45)
R_{sym} or R_{merge}	3.4 (16.9)	9.3 (35.9)	4.5 (15.2)	6.1 (30.7)	17.1 (36.5)	7.6 (33.1)	8.7 (32.2)	7.9 (30.6)
$I/\sigma I$	34.7 (9.3)	4.0 (2.0)	25.9 (10.2)	25.7 (5.4)	5.8 (2.7)	18.5 (4.4)	18.0 (4.8)	15.7 (4.9)
Completeness (%)	99.5 (99.2)	99.4 (99.4)	98.8 (96.9)	99.6 (99.3)	83.6 (78.6)	99.6 (99.7)	99.9 (100)	99.1 (96.3)
Redundancy	7.1 (7.2)	2.9 (2.8)	3.0 (3.0)	4.3 (4.4)	2.3 (2.1)	4.9 (4.9)	5.1 (5.1)	4.1 (4.0)
Refinement								
Resolution (Å)	27.7–1.5	42.5–1.5	22.7–1.5	26.4–1.8	39.0–2.75	41.0–1.5	45.0–1.70	29.0–1.45
Reflections (n)	18,424	8296	7884	16,865	413	51,198	35,529	56,325
R_{work}/R_{free}	13.3/17.7	14.1/19.0	11.5/19.2	19.8/25.2	21.1/26.6	11.7/14.9	11.9/15.6	12.5/15.6
Atoms (n)	1106	613	567	1609	2693	2214	2159	2207
Protein	933	515	473	1424	2688	1943	1906	1906
Ligand/ion	2			1	3	20	22	23
Water	171	98	94	184	2	251	231	278
B-factors	19.6	12.6	10.7	24.1	40.0	17.7	16.3	14.5
Protein	16.8	10.8	9.2	23.0	40.0	15.9	14.8	12.3
Ligand/ion	15.1			13.9	40.0	13.2	14.2	13.2
Water	34.8	22.0	18.3	33.2	40.0	32.0	29.1	29.6
Rmsd								
Bond lengths (Å)	0.024	0.026	0.024	0.023	0.008	0.034	0.029	0.029
Bond angles (°)	2.05	2.78	2.65	2.19	1.27	2.40	2.14	2.24
PDB ID	3POE	3PON	3POD	3POB	3POG	3POF	3POI	3POJ

PDB, Protein Data Bank; Rmsd, root-mean-square deviation.
[a] Highest resolution shell is shown in parenthesis.

change little upon collagen binding. The Ca^{2+} thus serves at least two roles: first it stabilizes the binding loops L5 and L9, and second, it coordinates the specific arrangement of acidic residues that contact Lys46 of MBL. This structure, therefore, provides a clear rationale for the Ca^{2+}-dependence of binding, a feature common to all lectin and classical pathway complexes.

Unexpectedly, the relative orientations of MBL and MASP are different from previous predictions, which were based primarily on mutagenesis of human MASP-1 (Teillet et al., 2008). In particular MBL is inverted relative to previous models and the collagen-like stem follows a different path across the MASP (Figure S2). Binding is stabilized by a combination of hydrogen bonds and hydrophobic contacts. In particular, Hyp44 of the trailing chain, forms two important water-mediated hydrogen bonds to the carbonyl group of Asp217 and the carboxylate of Asp216 (Figure 3D), probably accounting for the unique conformation observed in the crystal structure. These interactions would not be possible if Lys46 of the middle or trailing strand were to sit in the binding pocket, because a leucine residue would occupy the position of the hydroxyproline. Tyr225 of the MASP forms extensive hydrophobic interactions at the binding interface and its hydroxyl group forms a hydrogen bond with the backbone carbonyl of Leu47 of the leading chain of the collagen. His218 also participates in the hydrogen-bonding network, forming backbone contacts to the carbonyl of Gly45 of the trailing chain and the amide of Glu220 of the MASP. The latter interaction probably stabilizes the conformation of loop L5, which remains in close proximity to the collagen, thereby reducing solvent accessibility to the binding interface. The side chain of Glu220 in loop L5 is sandwiched between the side chain of Lys46 and the amide of Leu47 of the trailing chain and is partially buried at the interface (Figure 3D). Overall binding buries just 326 $Å^2$ of solvent-accessible collagen surface and 305 $Å^2$ of the MASP1, which is small for a protein/protein complex and smaller than the handful of protein/collagen

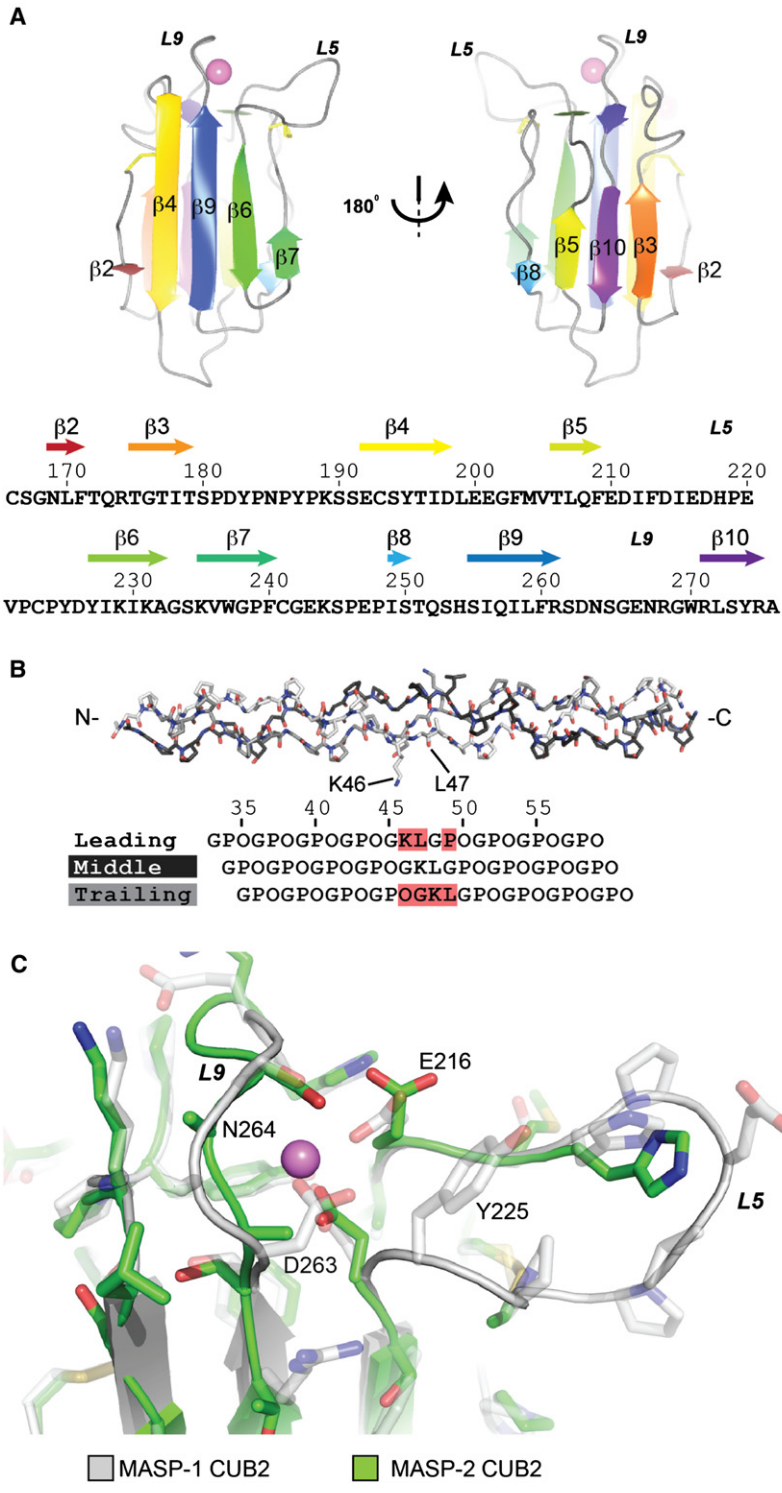

Figure 2. Structures of MASP-1 CUB2 and the Collagen-Like Peptide from MBL

(A) Structure of unbound MASP-1 CUB2 (crystal form 1, PDB: 3POE). Secondary structural elements are indicated, and the Ca^{2+} is shown in violet. Numbering is based on the mature MASP polypeptide.

(B) Structure of the unbound collagen-like peptide with the leading, middle and trailing strands in white, black, and gray, respectively (peptide 1, PDB 3PON). The sequence of the peptide is shown below the structure, to illustrate the stagger between each chain. Numbering is based on the mature rat MBL polypeptide. Residues involved in MASP binding are highlighted in red. Lys46 and Leu47 of the leading chain are indicated by arrows.

(C) Comparison of the Ca^{2+}-bound MASP-1 CUB2 domain (white) with the apo-MASP-2 CUB2 domain (green). In the apo-structure, loop L5 and some of the side chains in Loop L9 (MASP2 equivalents of Asp263 and Asn264) are absent in the density map likely due to flexibility, suggesting that Ca^{2+} stabilizes the CUB fold by reducing flexibility in loops L5 and L9. See also Figure S1.

complexes for which structures are available (Emsley et al., 2000; Zong et al., 2005; Hohenester et al., 2008; Carafoli et al., 2009).

The structure of the CUB-collagen complex explains previous data which show: the importance of Ca^{2+}, and the role of the essential lysine residue in MBL and ficolins (Girija et al., 2007; Wallis et al., 2004). It also explains the significance of residues tested by mutagenesis of human MASP-1 (Teillet et al., 2008). For example, the mutation Tyr225Ala completely disrupted binding to H-ficolin and reduced binding to MBL and L-ficolin significantly, whereas His218Ala reduced binding to all three proteins. Interestingly, Ser265Ala had relatively little effect, showing that loss of the hydrogen bond between Ser265 and Lys46 can be partially tolerated, presumably because the remaining two salt-bridges mediated by Glu216 and Asp263 are preserved.

Steric factors probably play an important role in determining the relative orientations of MBL and MASP. In the binding orientation, His218 and Tyr225 occupy a groove in the collagen formed from residues that make up the MASP-binding motif (OGKLGP) and make hydrogen bonds with the peptide backbone. Because the binding motif is present in all MBLs, ficolins, CL-K1 and C1q (Figure S2), this groove is likely to be a common feature. By contrast, residues forming the adjacent groove (that would be occupied in the alternative orientation) are variable in different family members and often bulky, so would exclude the MASP (Figure S2). For example, in human and rat MBLs, leucine and glutamine residues would block access to His218 and Tyr225.

Comparison of the structure of the complex with structures of the CUB2 domain in the absence of the collagen (CUB-Forms 1, 2A, and B; Table 1) reveals differences in the position of loop L5 (Figure 4A), consistent with significant but limited flexibility in the unbound MASP. In particular, the positions of Tyr225, His218, and Glu220, diverge by several angstroms. By contrast, these residues are essentially fixed in all complexes (MASP1 bound to

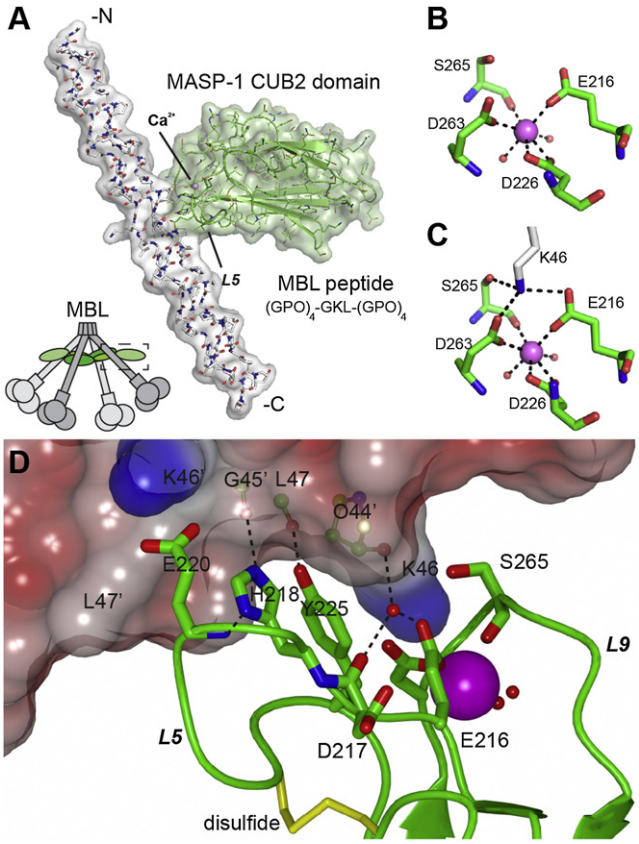

Figure 3. Structure of the Ca^{2+}-Dependent MBL/MASP Complex

(A) Crystal structure of MASP-1 CUB2 (green) bound to the MBL collagen-like peptide 1 (white) (PDB: 3POB). The CUB2 domain is located mainly on the outside of the cone created by the MBL subunits (left).

(B) The Ca^{2+}-binding site of the unbound CUB2 domain, showing the six coordinating ligands arranged in a tetragonal bipyramid. The Ca^{2+} is shown in violet, water molecules as red spheres, and ionic and electrostatic bonds by dotted lines.

(C) The same view of the CUB domain in the complex, showing the interaction with Lys46 of MBL.

(D) Close-up of the MBL/MASP interface. The electrostatic potential of the collagen is shown on a semitransparent surface representation with key structural elements represented as ball and sticks; binding residues of CUB2 (green) are shown as cylinders. Residue numbers of the MBL leading and trailing strands (with an apostrophe) are shown. See also Figure S2.

collagen, methylamine, ethylamine or the autoinhibited form; Table 1 and see below), because of packing of the collagen against Tyr225. Thus, the collagen locks the binding loops of the MASP against the collagen-like stem. Otherwise, there is little conformational change to the CUB or the collagen stem on association.

A Conserved Mode of Ca^{2+}-Dependent Binding in the Classical and Lectin Pathways

The mode of binding described here is likely to be the same in all activating complexes of the lectin and classical pathways. Lys46 of MBL is central to all interactions and binding residues are strictly conserved in the CUB2 domains of MASP-2 and C1r (Figures 4C and 4D; Figure S3). However, His218 and Tyr225 are substituted by alanine and leucine in C1s (Figure 4E), which

Table 2. Surface area (Å^2) of MBL buried upon complex formation

MBL residue	Leading	Trailing
Hyp44	0	54.2
Gly45	0	8.6
Lys46	106.5	32.2
Leu47	9.7	48.2
Gly48	0.1	0
Pro49	65.0	0
Hyp50	1.9	0

The total buried area is 326.4 Å^2. MBL, mannan-binding lectin.

does not bind to C1q (Phillips et al., 2009). Superimposition of MASP-1 CUB1 and CUB2 structures further demonstrates the similarity of the collagen-binding sites, whereby the side chains of the Ca^{2+}-coordinating residues Glu49, Asp102, and Ser104 substitute for Glu216, Asp263, and Ser265, respectively (Figure 4B; Figure S3). In addition, Tyr56 substitutes for Tyr225, but the histidine in loop L5 is missing. Instead, Phe103 of loop L9 and Tyr52 of loop L5 probably participate in binding to dictate the orientation of the collagen-like stem, consistent with previous mutagenesis data (Teillet et al., 2008).

The central features of the MBL-MASP structure are also remarkably similar to binding between vitamin B_{12}-bound gastric intrinsic factor and cubilin (another CUB-containing protein), revealing a common mechanism for Ca^{2+}-dependent CUB interactions (Andersen et al., 2010). In each case, binding is multivalent involving the interaction of a basic side chain to residues coordinating a Ca^{2+} within the CUB, with neighboring loops making additional contributions. The propensity of Ca^{2+}-binding CUB domains to bind in this way is further demonstrated in a crystal structure of the autoinhibited CUB domain of MASP-1 (CUB2-Form 3), in which a lysine side chain from each of the three domains present in the asymmetric unit penetrates into the binding pocket of its adjacent partner, mimicking the natural collagen/CUB interaction (Figure S3).

Structure Guided Inhibition of MASP Interactions

The binding pocket of the MASP represents an attractive potential target for small molecule inhibitors of complement activation by preventing assembly of activating complexes. To verify this concept we tested the inhibitory activities of small amines using a lectin pathway-specific assay. Remarkably, lysine inhibited complement activation in both human (Figure 5A) and mouse serum (Figure S4) with IC_{50} values of ~30 mM, whereas other amino acids (alanine, serine, and threonine) had little effect, at concentrations up to 400 mM. Lysine also inhibited binding between MBL and full-length MASP-1 (IC_{50} of ~50 mM); Figure S4), suggesting that complement inhibition was caused by dissociation of MBL/MASP complexes in serum. Inhibition of binding was not due to increasing ionic strength because addition of extra NaCl (up to 400 mM) above physiological ionic strength had little effect (Figure S4). To confirm the mechanism of inhibition, we cocrystallized the CUB2 domain with ethylamine and methylamine, which also inhibited MBL binding. In the resulting structures, both inhibitors occupy the lysine-binding pocket of the MASP, forming equivalent contacts to Glu216,

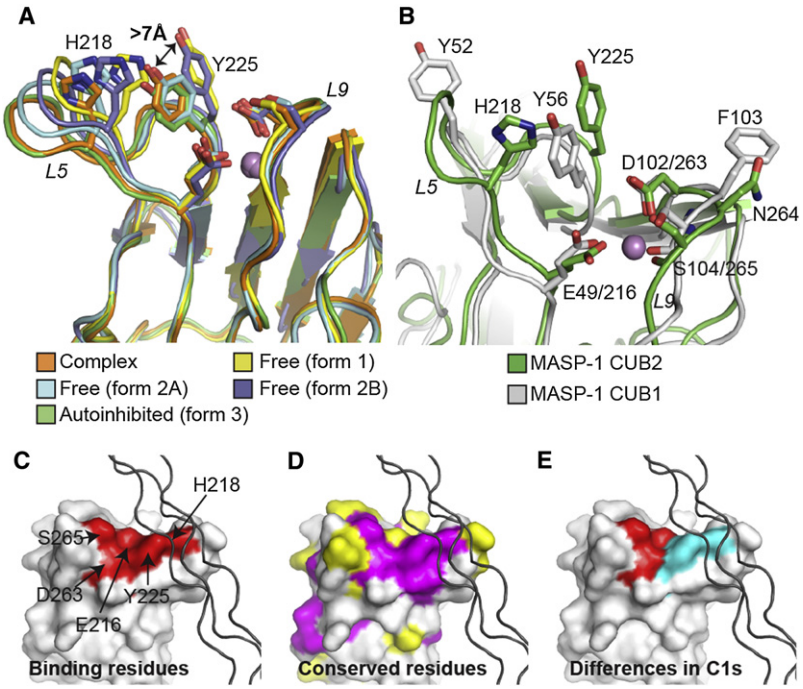

Figure 4. Conserved Mechanism of CUB-Collagen Interactions in the Lectin and Classical Pathways of Complement

(A) Comparison of collagen-bound MASP-1 CUB2 with four unbound structures (from crystal forms 1, 2A, 2B, and 3). Ca^{2+} and Ca^{2+}-coordinating residues are in equivalent positions. Different conformations of Loop L5, and Tyr225 in particular, reflect a significant flexibility.

(B) Superimposition of rat MASP-1 CUB2 and human MASP-1 CUB1 (PDB: 3DEM) (Teillet et al., 2008). The lysine-binding pocket is conserved reflecting a common mode of binding. Ca^{2+}-coordinating residues occupy equivalent positions, whereas differences in the binding loops L5 and L9 probably dictate the orientation of the collagen-like domain.

(C–E) Same view of the MBL/MASP complex in which: (C) binding residues are shown in red; (D) identical and conserved substitutions in human MASP-1, MASP-2, and C1r are shown in purple and yellow, respectively, and (E) binding residues that are the same in C1s are in red and those that are different are in blue. See also Figure S3.

Asp263, and Ser265, and packing against Tyr225 (Figure 5B; Figure S4), thus blocking the binding site.

DISCUSSION

Implications for Complement Activation

A variety of models have been proposed to explain the mechanism of complement activation. However, lack of structural information on the interactions between components has prevented a detailed description of the physical changes. Combining our MBL/MASP complex with the structure of the CUB1-EGF-CUB2 dimer of human or rat MASP (Feinberg et al., 2003; Teillet et al., 2008), reveals that the MASP domains take the form of the cross-bar of an uppercase letter "A," with each CUB2 domain holding a collagen-like stem to form the sides. By bridging separate stems, the MASP is receptive to changes imparted following engagement of a pathogen by MBL. However, the unexpected orientation of MBL relative to the MASP means that rather than converging at the N-terminus as predicted in previous models, instead the collagenous stems crossover and extend beyond the point of intersection (Figure 6A). Clearly, this would not be possible in a MBL/MASP complex, because the stems are bound together at the base. Thus, one or both components must change conformation when they associate, imparting strain to the resulting zymogen complex (Figure 6B). Given the rigidity of the stems, binding probably leads to distortion of the MASP, via flexion of the EGF-CUB2 junction. This junction is likely to be flexible because it is susceptible to proteolysis (Wallis and Dodd, 2000) and the domain interface is small, unlike the CUB1-EGF junction, which is fixed through extensive hydrophobic packing (Feinberg et al., 2003; Teillet et al., 2008). When MBL engages with a pathogen, release of the tension would lead to extension of the EGF-CUB2 junction as the stems splay apart, pulling the SP domains together to allow reciprocal activation (Figure 6C). This simple model only requires changes to the angle between the stems of MBL and flexion/extension of the EGF-CUB2 junction of the MASP; the MBL/MASP contacts remain fixed. Importantly, it is compatible with kinetic and biochemical data, which also suggest that the MASP becomes primed for activation when it binds to MBL (Chen and Wallis, 2004; Venkatraman Girija et al., 2010).

The MBL/MASP Interface as a Target for Inhibitors of Complement Activation

Inhibition of the lectin pathway has potential for the treatment of complement-dependent disorders and ischemia-reperfusion injury following cardiac arrest or stroke (Schwaeble et al., 2011). The C1 complex is also an important drug target because of its pathogenic role in various neurodegenerative disorders including Alzheimer's disease (Tenner and Fonseca, 2006). The structural insight described here provides a starting point for the design of such therapeutics. Although the affinities of the small amine inhibitors identified here is low, high-affinity compounds can potentially be developed using a fragment-based approach, in which two or more small compounds are combined (Murray and Blundell, 2010). Notably, although the binding site itself is highly conserved, it is surrounded by variable residues which would allow specificity to be introduced into larger inhibitors (Figure 5C). Such inhibitors would block complement at its earliest stage, before amplification, and would not compromise other immunological processes.

EXPERIMENTAL PROCEDURES

Production and Refolding of the MASP-1 CUB2 Domain

The cDNA encoding rat MASP-1 CUB2 (E165-A277) was cloned into pET28A (Novagen) and transformed into *E. coli* BL21 DE3. Production was induced by addition of IPTG (1 mM) at an OD_{595} of 0.8 in 2 × YT medium at 37°C. After 4 hr, cells were lysed by sonication in Bugbuster reagent (40 ml/L of culture; Novagen) containing a protease inhibitor cocktail (1 tablet/40 ml of culture

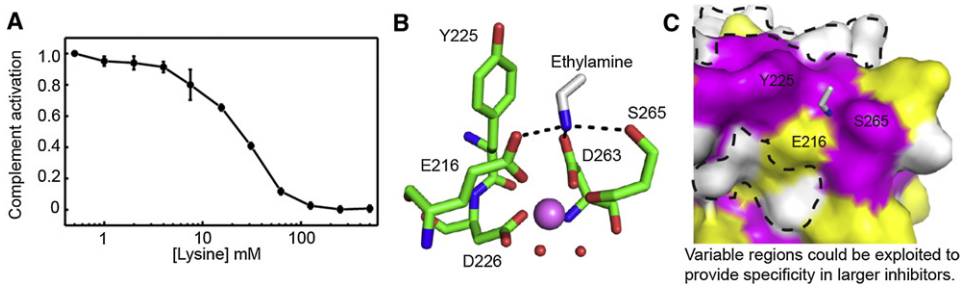

Figure 5. Inhibition of Complement Activation by Small Amines

(A) Inhibition of the lectin pathway of complement activation by lysine measured by deposition of the membrane-attack complex. Data are expressed relative to the activation in the absence of lysine. Error bars represent the difference between duplicate measurements. The IC_{50} from three independent experiments was 25 ± 3 mM.

(B and C) Structure of the lysine-binding pocket of MASP-1 CUB2 bound to ethylamine; (C) Conserved residues in human MASP-1, MASP-2, and C1r (purple for identical and yellow for similar) at the binding interface are surrounded by patches of nonconserved residues (white; contoured by dotted lines). See also Figure S4.

suspension; Roche). Inclusion bodies were washed twice with 1:10 diluted Bugbuster mix, 2 M urea in 50 mM Tris/HCl pH 8.0 containing 0.5 M NaCl and 1 mM EDTA and were solubilized to a final concentration of 2 mg/ml in 8M urea in 50 mM Tris/HCl pH 8.0, containing 5 mM DTT. The CUB domain was refolded by drop dilution into 50 mM Tris/HCl, pH 8.5, containing 240 mM NaCl, 10 mM KCl, 2 mM $MgCl_2$, 2 mM $CaCl_2$, 0.4 M sucrose, and 1 mM DTT so that the final protein concentration was 0.1 mg/ml. After 3 days at 4°C, the sample was bound to a Q-Sepharose column (20 mL) equilibrated with 25 mM Tris/HCl at pH 8.0, containing 25 mM NaCl and eluted using a gradient of NaCl (25 mM to 1 M over 40 ml). It was further purified by gel filtration (16/60 Superdex 75; GE Healthcare) in 10 mM Tris buffer (pH 7.5) containing 10 mM NaCl and 2 mM $CaCl_2$.

Proteins and Peptides

Rat MBL-A (referred to as MBL) and MASP-1ent (referred to as MASP-1), a modified form of MASP-1 that cannot autoactivate were produced and purified as described previously (Chen and Wallis, 2004; Wallis and Drickamer, 1999). Two collagen peptides were made by Pepceuticals Ltd. Peptide 1 is $Ac(GPO)_4$-GKL-$(GPO)_4NH_2$ and peptide 2 is $Ac(GPO)_3$-GKL-$(GPO)_4NH_2$.

Crystallization and Structure Determination

All crystals were grown using the sitting-drop method by mixing equal volumes (1.2 + 1.2 μL) of protein and reservoir solution. They were transferred to reservoir solution containing 20% glycerol before cryoprotection in liquid nitrogen, and were maintained at 100 K during data collection. Diffraction data were collected at ESRF and Diamond Light Source and were processed with XDS (Kabsch, 1993). Phases were determined by molecular replacement with Phaser and models were optimized using cycles of manual refinement with Coot and maximum likelihood refinement in Refmac5, part of the CCP4 software suite (Collaborative Computational Project, 1994). For the complex, CUB domain (5 mg/ml; 0.38 μM) containing a 1.5-fold molar excess of trimeric peptide was mixed with 28% PEG 8000, 50 mM Tris/HCl, pH 8.0, and 4 mM $CaCl_2$. Phases were determined using structures of the free components as search models.

The CUB2 domain alone was crystallized in three different conditions to give different crystal forms (Table 1). Reservoir solutions were: (1), 24% PEG 8 K in 50 mM Tris/HCl, pH 9.0 containing 20 mM $CaCl_2$; (2), 1.5 M lithium sulfate in 100 mM Tris, pH 8.5; and (3), 24% PEG 8 K in 50 mM Tris/HCl, pH 9.0 containing 200 mM $MgCl_2$. The initial structure (crystal form 1) was determined using the human MASP-1 CUB2 module as a search model (Protein Data Bank [PDB] ID: 3DEM) (Teillet et al., 2008), and was refined to 1.5 Å resolution (Table 1). The identity of the Ca^{2+} was verified by its anomalous signal using CuKα radiations from an in-house X ray source. We found a second Ca^{2+} ion in the anomalous signal coordinated by Ser190, Glu192, and four water molecules. This region of the protein is usually at the interface with the EGF module in the full-length MASP, which would not permit Ca^{2+} binding, so its presence is likely due to the high concentration of Ca^{2+} in the crystallization buffer. Crystal form 2 contained two CUB molecules in the asymmetric unit (forms 2A and 2B; Table 1). Similar crystallization conditions were used for the complexes with methylamine, ethylamine, and lysine. In each case, only one conformation of CUB2 was seen bound to the amine. There were three molecules in the asymmetric unit of crystal form 3, called the autoinhibited form, which were almost identical (Table 1). Complexes of CUB2 bound to ethylamine, methylamine, and lysine were crystallized in buffer condition 2, supplemented with 1 M amine (Sigma). Although crystals grew in the presence lysine and novel density was observed in the binding pocket, lysine was not resolved in the resulting structure, probably reflecting multiple binding conformations.

Both collagen peptides were crystallized using a reservoir solution of 1.6 M ammonium sulfate in 100 mM MES, pH 6.0, but yielded different crystal forms. Crystals of collagen peptide 1 and 2 each diffracted to 1.5 Å resolution and the phases were determined by molecular replacement using the Gly-Pro-Hyp collagen peptide structure as a search model (PDB ID: 1CAG) (Bella et al., 1994). The C-terminal end of peptide 1 of the trailing chain is not well resolved and shows higher temperature factor due to the absence of neighboring chains.

Gel Filtration

Gel filtration was carried out on a 16/60 Superdex 200 column (GE Healthcare) in 50 mM Tris/HCl pH 7.4, containing 150 mM NaCl at a flow rate of 1 ml/min.

Isothermal Titration Calorimetry

The CUB2 domain (114 μM) pretreated by dialysis to remove Ca^{2+} was titrated with freshly prepared 2 mM $CaCl_2$ in the same batch of assay buffer in the cell of a VP-isothermal titration calorimeter (Microcal) equilibrated at 25°C. Data were fitted to a 1:1 binding model using the Origin software supplied. Binding was measured under low "c-value" conditions (where the concentration of the protein in the cell is lower than that of the K_D). The stoichiometry was fixed at 1 (based on the crystal structure) and the K_A and ΔH variables were allowed to float.

Surface Plasmon Resonance

MBL (0.025 mg/ml) was immobilized onto the surface of a GLM sensor chip (BioRad; ~10,000 response units) at pH 4.5, using amine-coupling chemistry. Binding to CUB2 was measured using a ProteOn XPR36 (BioRad) in 10 mM Tris/HCl pH 7.4, containing 140 mM NaCl, 5 mM Ca^{2+}, and 0.005% Tween-20 at 25°C, and at a flow rate of 25 μL/min. For inhibition assays, MBL was immobilized on to a CM-5 sensor chip (GE Healthcare; ~14,000 response units) and binding was measured using a Biacore 2000 (GE Healthcare). MASP-1 (100 nM) was premixed with inhibitor and flowed over the chip surface at a rate of 5 μL/min at 25°C for 10 min. Changes in response units caused by differences in sample composition were subtracted from all data. MASP-1 CUB2 was immobilized on to the chip at pH 4.0 (1000–2000 response units), in the same way as MBL. Binding to peptide 1 was measured at 20°C using a flow rate of 5 μl/min.

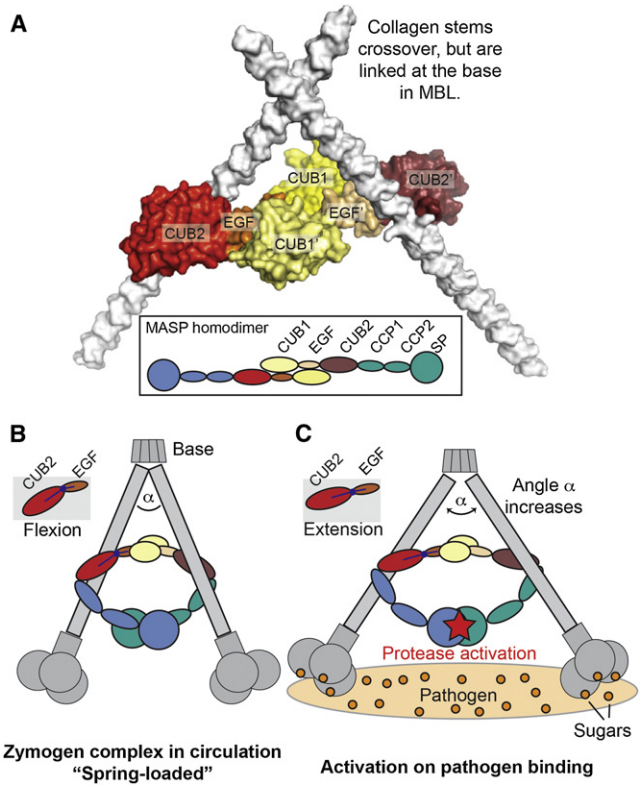

Figure 6. Structural Basis of Complement Activation in the Lectin Pathway

(A) Superimposition of the structures of the MBL/MASP-1 complex with the human CUB1-EGF-CUB2 (PDB: 3DEM) and extension of the collagen-like stems to their full-length (59 residues) shows that the stems crossover, which is not possible in intact MBL.

(B) In the zymogen complex, MBL and/or MASP must undergo conformational changes on binding. The simplest way is through flexion of the EGF-CUB2 junction of the MASP, creating a "spring-loaded" structure.

(C) Activation of the complex occurs upon binding to a pathogen. Release of the strain causes the stems to splay apart and pulls the SP domains of the MASP into alignment to allow reciprocal cleavage and activation. In this model, only the angle between collagen-like stems (α) and flexion/extension of the EGF-CUB2 junction is necessary for activation; the MBL/MASP contacts are fixed.

Complement Activation Assays

Lectin pathway specific complement activation in human serum was measured using the Wieslab MBL pathway kit (Euro-Diagnostica). The lectin pathway is functional, even under conditions of high ionic strength (1 M NaCl) (Petersen et al., 2001).

Complement activation in mouse serum was measured by deposition of complement component C3c. Nunc MaxiSorb microtiter plates were coated with 2 ug of mannan per well in 100 mM sodium bicarbonate buffer, pH 9.6. After overnight incubation at 4°C, wells were blocked with 0.1% bovine serum albumin in binding buffer (10 mM Tris/HCl, 140 mM NaCl, pH 7.4) for 2 hr at room temperature. The wells were then washed three times with binding buffer containing 0.05% Tween-20 and 5 mM $CaCl_2$. Mouse serum diluted 1:100 in 4 mM sodium barbitone buffer, pH 7.4, containing 145 mM NaCl, 2 mM $CaCl_2$, 1 mM $MgCl_2$, containing inhibitor was added to the plates and incubated overnight at 4°C. After three additional washes, bound C3c was detected using rabbit anti-C3c antibody (Dako) and alkaline phosphatase conjugated goat anti-rabbit IgG (Sigma) using Sigma FAST *p*-nitrophenyl phosphate substrate (Sigma).

ACCESSION NUMBERS

Coordinates have been deposited in the Protein Data Base with accession codes 3POB, 3POD, 3POE, 3POF, 3POG 3POI, 3POJ, and 3PON.

SUPPLEMENTAL INFORMATION

Supplemental Information includes four figures and can be found with this article online at doi:10.1016/j.str.2011.08.014.

ACKNOWLEDGMENTS

The authors thank Gordon C.K. Roberts, Colin Kleanthous, Mark H. Ginsberg, and Helen O'Hare for critical reading of the manuscript. The authors also thank beamline scientists at the ESRF and Diamond Light Source and the UK Midlands Block Allocation Groups mx310 for DLS and mx1218 for ESRF (A.R.G.). This work was supported by the Research Councils UK (R.W. and D.M.), MRC grant G0501425 (R.W.), and Wellcome Trust grant 087848 (A.R.G.).

Received: June 10, 2011
Revised: August 4, 2011
Accepted: August 17, 2011
Published: November 8, 2011

REFERENCES

Andersen, C.B., Madsen, M., Storm, T., Moestrup, S.K., and Andersen, G.R. (2010). Structural basis for receptor recognition of vitamin-B(12)-intrinsic factor complexes. Nature *464*, 445–448.

Bella, J., Eaton, M., Brodsky, B., and Berman, H.M. (1994). Crystal and molecular structure of a collagen-like peptide at 1.9 A resolution. Science *266*, 75–81.

Botto, M., Dell'Agnola, C., Bygrave, A.E., Thompson, E.M., Cook, H.T., Petry, F., Loos, M., Pandolfi, P.P., and Walport, M.J. (1998). Homozygous C1q deficiency causes glomerulonephritis associated with multiple apoptotic bodies. Nat. Genet. *19*, 56–59.

Carafoli, F., Bihan, D., Stathopoulos, S., Konitsiotis, A.D., Kvansakul, M., Farndale, R.W., Leitinger, B., and Hohenester, E. (2009). Crystallographic insight into collagen recognition by discoidin domain receptor 2. Structure *17*, 1573–1581.

Chen, C.B., and Wallis, R. (2001). Stoichiometry of complexes between mannose-binding protein and its associated serine proteases. Defining functional units for complement activation. J. Biol. Chem. *276*, 25894–25902.

Chen, C.B., and Wallis, R. (2004). Two mechanisms for mannose-binding protein modulation of the activity of its associated serine proteases. J. Biol. Chem. *279*, 26058–26065.

Collaborative Computational Project, Number 4. (1994). The CCP4 Suite: Programs for Protein Crystallography. Acta Crystallogr. *50*, 760–763.

Dobó, J., Harmat, V., Beinrohr, L., Sebestyén, E., Závodszky, P., and Gál, P. (2009). MASP-1, a promiscuous complement protease: structure of its catalytic region reveals the basis of its broad specificity. J. Immunol. *183*, 1207–1214.

Drickamer, K., and Taylor, M.E. (1993). Biology of animal lectins. Annu. Rev. Cell Biol. *9*, 237–264.

Emsley, J., Knight, C.G., Farndale, R.W., Barnes, M.J., and Liddington, R.C. (2000). Structural basis of collagen recognition by integrin alpha2beta1. Cell *101*, 47–56.

Feinberg, H., Uitdehaag, J.C., Davies, J.M., Wallis, R., Drickamer, K., and Weis, W.I. (2003). Crystal structure of the CUB1-EGF-CUB2 region of mannose-binding protein associated serine protease-2. EMBO J. *22*, 2348–2359.

Fujita, T., Matsushita, M., and Endo, Y. (2004). The lectin-complement pathway—its role in innate immunity and evolution. Immunol. Rev. *198*, 185–202.

Garred, P., Madsen, H.O., Balslev, U., Hofmann, B., Pedersen, C., Gerstoft, J., and Svejgaard, A. (1997). Susceptibility to HIV infection and progression of AIDS in relation to variant alleles of mannose-binding lectin. Lancet *349*, 236–240.

Girija, U.V., Dodds, A.W., Roscher, S., Reid, K.B., and Wallis, R. (2007). Localization and characterization of the mannose-binding lectin (MBL)-associated-serine protease-2 binding site in rat ficolin-A: equivalent binding sites within the collagenous domains of MBLs and ficolins. J. Immunol. *179*, 455–462.

Gulla, K.C., Gupta, K., Krarup, A., Gal, P., Schwaeble, W.J., Sim, R.B., O'Connor, C.D., and Hajela, K. (2010). Activation of mannan-binding lectin-associated serine proteases leads to generation of a fibrin clot. Immunology *129*, 482–495.

Harmat, V., Gál, P., Kardos, J., Szilágyi, K., Ambrus, G., Végh, B., Náray-Szabó, G., and Závodszky, P. (2004). The structure of MBL-associated serine protease-2 reveals that identical substrate specificities of C1s and MASP-2 are realized through different sets of enzyme-substrate interactions. J. Mol. Biol. *342*, 1533–1546.

Hohenester, E., Sasaki, T., Giudici, C., Farndale, R.W., and Bächinger, H.P. (2008). Structural basis of sequence-specific collagen recognition by SPARC. Proc. Natl. Acad. Sci. USA *105*, 18273–18277.

Hurwitz, S. (1996). Homeostatic control of plasma calcium concentration. Crit. Rev. Biochem. Mol. Biol. *31*, 41–100.

Kabsch, W. (1993). Automatic processing of rotation diffraction data from crystals of initially unknown symmetry and cell constants. J. Appl. Crystallogr. *26*, 795–800.

Kilpatrick, D.C. (2002). Mannan-binding lectin: clinical significance and applications. Biochim. Biophys. Acta *1572*, 401–413.

Krarup, A., Wallis, R., Presanis, J.S., Gál, P., and Sim, R.B. (2007). Simultaneous activation of complement and coagulation by MBL-associated serine protease 2. PLoS ONE *2*, e623.

Megyeri, M., Makó, V., Beinrohr, L., Doleschall, Z., Prohászka, Z., Cervenak, L., Závodszky, P., and Gál, P. (2009). Complement protease MASP-1 activates human endothelial cells: PAR4 activation is a link between complement and endothelial function. J. Immunol. *183*, 3409–3416.

Mullighan, C.G., Heatley, S.L., Danner, S., Dean, M.M., Doherty, K., Hahn, U., Bradstock, K.F., Minchinton, R., Schwarer, A.P., Szer, J., and Bardy, P.G. (2008). Mannose-binding lectin status is associated with risk of major infection following myeloablative sibling allogeneic hematopoietic stem cell transplantation. Blood *112*, 2120–2128.

Murray, C.W., and Blundell, T.L. (2010). Structural biology in fragment-based drug design. Curr. Opin. Struct. Biol. *20*, 497–507.

Neth, O., Hann, I., Turner, M.W., and Klein, N.J. (2001). Deficiency of mannose-binding lectin and burden of infection in children with malignancy: a prospective study. Lancet *358*, 614–618.

Petersen, S.V., Thiel, S., Jensen, L., Steffensen, R., and Jensenius, J.C. (2001). An assay for the mannan-binding lectin pathway of complement activation. J. Immunol. Methods *257*, 107–116.

Phillips, A.E., Toth, J., Dodds, A.W., Girija, U.V., Furze, C.M., Pala, E., Sim, R.B., Reid, K.B., Schwaeble, W.J., Schmid, R., et al. (2009). Analogous interactions in initiating complexes of the classical and lectin pathways of complement. J. Immunol. *182*, 7708–7717.

Rooryck, C., Diaz-Font, A., Osborn, D.P., Chabchoub, E., Hernandez-Hernandez, V., Shamseldin, H., Kenny, J., Waters, A., Jenkins, D., Kaissi, A.A., et al. (2011). Mutations in lectin complement pathway genes COLEC11 and MASP1 cause 3MC syndrome. Nat. Genet. *43*, 197–203.

Schwaeble, W., Dahl, M.R., Thiel, S., Stover, C., and Jensenius, J.C. (2002). The mannan-binding lectin-associated serine proteases (MASPs) and MAp19: four components of the lectin pathway activation complex encoded by two genes. Immunobiology *205*, 455–466.

Schwaeble, W.J., Lynch, N.J., Clark, J.E., Marber, M., Samani, N.J., Ali, Y.M., Dudler, T., Parent, B., Lhotta, K., Wallis, R., et al. (2011). Targeting of mannan-binding lectin-associated serine protease-2 (Masp2) confers a significant degree of protection from myocardial and gastrointestinal ischemia/reperfusion injury. Proc. Natl. Acad. Sci. USA *108*, 7523–7528.

Sumiya, M., Super, M., Tabona, P., Levinsky, R.J., Arai, T., Turner, M.W., and Summerfield, J.A. (1991). Molecular basis of opsonic defect in immunodeficient children. Lancet *337*, 1569–1570.

Teillet, F., Gaboriaud, C., Lacroix, M., Martin, L., Arlaud, G.J., and Thielens, N.M. (2008). Crystal structure of the CUB1-EGF-CUB2 domain of human MASP-1/3 and identification of its interaction sites with mannan-binding lectin and ficolins. J. Biol. Chem. *283*, 25715–25724.

Tenner, A.J., and Fonseca, M.I. (2006). The double-edged flower: roles of complement protein C1q in neurodegenerative diseases. Adv. Exp. Med. Biol. *586*, 153–176.

Venkatraman Girija, U., Furze, C., Toth, J., Schwaeble, W.J., Mitchell, D.A., Keeble, A.H., and Wallis, R. (2010). Engineering novel complement activity into a pulmonary surfactant protein. J. Biol. Chem. *285*, 10546–10552.

Wallis, R., and Drickamer, K. (1999). Molecular determinants of oligomer formation and complement fixation in mannose-binding proteins. J. Biol. Chem. *274*, 3580–3589.

Wallis, R., and Dodd, R.B. (2000). Interaction of mannose-binding protein with associated serine proteases: effects of naturally occurring mutations. J. Biol. Chem. *275*, 30962–30969.

Wallis, R., Mitchell, D.A., Schmid, R., Schwaeble, W.J., and Keeble, A.H. (2010). Paths reunited: Initiation of the classical and lectin pathways of complement activation. Immunobiology *215*, 1–11.

Wallis, R., Shaw, J.M., Uitdehaag, J., Chen, C.B., Torgersen, D., and Drickamer, K. (2004). Localization of the serine protease-binding sites in the collagen-like domain of mannose-binding protein: indirect effects of naturally occurring mutations on protease binding and activation. J. Biol. Chem. *279*, 14065–14073.

Zong, Y., Xu, Y., Liang, X., Keene, D.R., Höök, A., Gurusiddappa, S., Höök, M., and Narayana, S.V. (2005). A 'Collagen Hug' model for Staphylococcus aureus CNA binding to collagen. EMBO J. *24*, 4224–4236.